

## Article

# Investigation of Porous Ceramic Structures Based on Hydroxyapatite and Wollastonite with Potential Applications in the Field of Tissue Engineering

Andraia Cucuruz <sup>1,\*</sup>, Cristina-Daniela Ghițulică <sup>2</sup>, Georgeta Voicu <sup>2</sup>, Cătălina-Alexandra Bogdan <sup>1</sup>, Vasilica Dochiu <sup>1</sup> and Roxana Cristina Popescu <sup>1,3</sup>

<sup>1</sup> Department of Bioengineering and Biotechnology, Faculty of Medical Engineering, National University of Science and Technology Politehnica, 011061 Bucharest, Romania;

bogdanalexandracatalina@yahoo.com (C.-A.B.); dochiu99@gmail.com (V.D.);

roxana.popescu1108@upb.ro (R.C.P.)

<sup>2</sup> Department of Science and Engineering of Oxide Materials and Nanomaterials, Faculty of Chemical Engineering and Biotechnologies, National University of Science and Technology Politehnica, 011061 Bucharest, Romania; cristina.ghitulica@upb.ro (C.-D.G.); georgeta.voicu@upb.ro (G.V.)

<sup>3</sup> Department of Life and Environmental Physics, National Institute for R&D in Physics and Nuclear Engineering-Horia Hulubei, 077125 Magurele, Romania

\* Correspondence: andraia.cucuruz@upb.ro

**Abstract:** Bioceramics are the most promising materials used for hard tissue reconstruction. In this study, wollastonite/hydroxyapatite (HAp/WS)-type composite ceramic structures were synthesized with the aim of reaching a material with improved properties for use in bone tissue regeneration. The scaffolds were synthesized using a foam replica method, starting from ceramic powders with different mass ratios. These were subsequently studied and compared to identify the ideal mass ratio in terms bioactive character, appropriate mechanical properties, but also microstructural influence. The results indicate that all of the samples showed a highly porous microstructure with interconnected pores and high mineralization after 21 days of immersion in SBF. The porous structures with 90% and 70% mass contents of hydroxyapatite presented a well-defined structure and the highest values of mechanical compressive strength. Biocompatibility evaluation showed that osteoblast-like cells are able to penetrate the inner volume of the structures, exhibiting a biocompatible behavior in terms of morphological features and viability following 7 days of incubation. All results show that the porous composite ceramics with 90% and 70% mass contents of hydroxyapatite are promising materials for bone tissue regeneration.

**Keywords:** wollastonite; hydroxyapatite; scaffolds; ceramic; bone tissue regeneration



**Citation:** Cucuruz, A.; Ghițulică, C.-D.; Voicu, G.; Bogdan, C.-A.; Dochiu, V.; Popescu, R.C. Investigation of Porous Ceramic Structures Based on Hydroxyapatite and Wollastonite with Potential Applications in the Field of Tissue Engineering. *Ceramics* **2023**, *6*, 2333–2351. <https://doi.org/10.3390/ceramics6040143>

Academic Editor: Francesco Baino

Received: 20 October 2023

Revised: 5 December 2023

Accepted: 6 December 2023

Published: 8 December 2023



**Copyright:** © 2023 by the authors. Licensee MDPI, Basel, Switzerland. This article is an open access article distributed under the terms and conditions of the Creative Commons Attribution (CC BY) license (<https://creativecommons.org/licenses/by/4.0/>).

## 1. Introduction

In recent years, the medical field has been in constant change thanks to recent technological advances that have revolutionized the diagnosis and treatment of various diseases; these advances have provided opportunities for a good understanding of the complexity of biological processes and a functional understanding of the human body, thus improving the materials used in this domain. Consequently, a new approach in maintaining the integrity and functionality of the human body involves biomedical engineering. Due to significant advances in research, health and technology, biomedical engineering is an interdisciplinary subject in high demand that deals with the research and identification of the most suitable materials to improve human life. One of the branches of biomedical engineering is tissue engineering, which deals with the reconstruction of destroyed organs or tissues. Tissue engineering uses a porous structure, together with cells and growth factors, for the regeneration of tissues or organs damaged or destroyed by various pathological factors, and represents an alternative to tissue or organ transplants [1–3].

A multitude of natural and synthetic materials have been investigated so far; among these, bioceramics are the most promising materials used for hard tissue reconstruction. In the selection of such bioceramics in medical applications, the following must be considered: their ability to form a strong interfacial bonds with the host tissue; their good mineralization process; and bioceramics that are bioactive or bioresorbable. These abilities fulfill the necessary requirements to be employed in obtaining porous structures, which are the most used biomaterials in bone substitution or regeneration [3,4].

One of the most employed ceramic materials in tissue engineering for bone tissue, from the class of calcium phosphates, is hydroxyapatite. It has a similar structure and chemical composition to the inorganic part of natural bone and dentin. Hydroxyapatite is biocompatible, bioactive, chemically stable, osteoconductive and has applications in tissue engineering for the restoration of bone defects, and also in controlled drug release, dental implants, and as a covering material for some orthopedic implants or as a matrix for bone cements intended for filling bone defects [5,6].

Another material successfully used in biomedical bone tissue regeneration is wollastonite ( $\text{CaSiO}_3$ ), a material from the class of calcium silicates. Wollastonite is found in two polymorphic forms:  $\beta$ -wollastonite, corresponding to low temperatures, and above  $1124^\circ\text{C}$ , which passes into the  $\alpha$ -wollastonite phase, formed at temperatures up to  $1454^\circ\text{C}$  [7,8]. In the medical field, the  $\beta$  polymorphic form is preferred for use, due to the phase arrangement of its two constituent components, which leads to an increase in the mechanical and chemical properties of the material [9,10].

$\beta$ -wollastonite is characterized by a high bioactivity, and thus it is used to obtain scaffolds intended for tissue engineering of bone tissue because it stimulates the formation of a layer of hydroxyapatite on the surface of this structure, both *in vitro* and *in vivo* [7].

In recent years, hydroxyapatite has been combined with calcium silicates to achieve materials with a much more pronounced bioactive character due to the presence of silicon dioxide in their composition, which initiates and supports the biological and chemical processes of new bone formation by releasing an optimal concentration of ions that favors the proliferation and differentiation of pre-osteoblasts [11–13].

Such HAp/WS-based systems have been investigated by other researchers, according to literature studies [11,13,14], and the following findings have been reported:

- Kaili Lin and co-workers reported in 2011, that they obtained composite ceramics based on hydroxyapatite and wollastonite with a HAp:WS ratio from 10:90 to 90:10. The powders were obtained through a double coprecipitation process, while the ceramic structures were achieved with hot isostatic pressing. They reported that by increasing the WS content, the linear shrinkage of the composite ceramics decreased, while the porosity increased. Also, the flexural strengths of the sintered samples increased from  $98.06 \pm 3.27$  to  $221.30 \pm 15.69$  MPa when the amount of WS was increased. The dissolution rate and bioactivity of the HAp/WS composites were strongly dependent on the WS content, and increased with increasing amounts of WS. Regarding MSC activity on composite ceramics, these researchers reported an improvement compared to simple HAp bioceramics, especially for samples with 30% WS content.
- Sanosh Kunjalukkal Padmanabhan and co-workers in 2012 obtained porous structures based on hydroxyapatite and wollastonite with a replication method using synthesized HAp powder and commercial WS powder. According to the reported data, all of the porous structures showed a porosity of around 90% and a pore size greater than  $500\ \mu\text{m}$ . The results showed that with the increase in WS content in the composition, the linear shrinkage of the composite ceramics decreased, and the porosity was not influenced. In contrast, the mechanical compressive strengths of the samples increased from  $0.51 \pm 0.14$  to  $0.62 \pm 0.11$  and  $1.02 \pm 0.16$  MPa when adding 25 and 50% WS, respectively. More than 50% WS powder in the composition of the samples resulted in a decrease in strength to  $0.67 \pm 0.14$  MPa. Also, the porous structures exhibited

- excellent bioactive and resorption properties in biological solutions compared to basic HAp structures. These properties were strongly influenced by the WS content.
- R. Morsy and collaborators reported in 2015 that they obtained composite ceramic powders based on HAp/WS in ratios of 10:90 to 90:10, through a two-stage coprecipitation method; the reaction was carried out at 100 °C for 2 h, and calcination occurred at 800 °C. As reported, the method led to the formation of HAp/WS composite ceramic powders with controlled proportions and agglomerated particles with sizes smaller than 1 µm.

Starting from the mentioned literature studies, the authors of this study aimed to obtain new porous ceramic structures based on HAp/WS with potential applications in bone tissue engineering. The physico-chemical characterization of the samples was completed through an initial *in vitro* biological assessment performed on osteoblast-like cells. In order to study the mechanical, bioactive and biodegradation properties of the porous composite ceramic structures based on hydroxyapatite and wollastonite, the first step was to obtain, via the coprecipitation method, the composite ceramic powders in different mass ratios (10:90, 30:70, 50:50, 70:30 and 90:10); through comparison with the data reported in the specialized literature, the reaction temperature was maintained at 80 °C to obtain the powders during synthesis, in order to avoid the evaporation of the reaction water. The dry precipitates obtained were subjected to the thermal treatment of calcination at a temperature of 1000 °C, compared to the temperatures mentioned in the specialized literature. Studies showed that this temperature is optimal for the formation of both the hydroxyapatite and the wollastonite phases [15–19], after which the cooling was carried out at room temperature overnight. Composite ceramic powders were later used to obtain porous structures by the method of replicating a polyurethane sponge. The curve of the thermal treatment for the combustion of the polymer sponge and the subsequent sintering process was different from those reported in the mentioned literature studies. The authors of this research study selected a longer heat treatment time; thus, for the burning of the sponge, a heating rate of 1 °C/min was applied up to a temperature of 400 °C (according to the thermal analysis carried out on the polyurethane sponge in which it was observed that burning of the organic component in the proportion of 90% of the mass occurred at temperatures between 250 and 400 °C), which was maintained for 3 h for a slow process of burning the polymer sponge; this was carried out to avoid tensioning the ceramic structure. Later, the temperature was increased at a rate of 5 °C/min up to 1200 °C and was maintained for 3 h for a good sintering process of the porous structures. These structures were subsequently studied and compared to identify the ideal mass ratio related to bioresorbable and bioactive characteristics, but also regarding the microstructural influence. Also, the porous ceramic structures were investigated from the biocompatibility point of view through *in vitro* tests to assess their ability to support the penetration of osteoblast-like cells into the volume, as well as their adherence and growth.

By investigating such porous composite ceramic structures, we want to bring more information to support their use in the field of tissue engineering; however, this depends a lot on the type of bone structure such materials are going to replace. Thus, we consider that providing more information will make the selection of an ideal composition much easier, and also the synthesis route that is suitable for a type of bone structure.

## 2. Materials and Methods

### 2.1. Materials

In order to synthesize the composite ceramic powders based on hydroxyapatite and wollastonite a facile *in situ*, a coprecipitation method was used, briefly described by R. Morsy et al. [13]. In this research, we used calcium hydroxide ( $\text{Ca}(\text{OH})_2$ ) (Chimopar Trading SRL, Bucharest, Romania), phosphoric acid 85% ( $\text{H}_3\text{PO}_4$ ) (SC Silal Trading SRL, Bucharest, Romania), calcium nitrate tetrahydrate 99–203% ( $\text{Ca}(\text{NO}_3)_2 \cdot 4\text{H}_2\text{O}$ ) (Sigma Aldrich, Berlin, Germany), sodium silicate solution nonahydrate ( $\text{Na}_2\text{SiO}_3 \cdot 9\text{H}_2\text{O}$ ) (Sigma

Aldrich, Berlin, Germany), ammonia 25% (NH<sub>3</sub>) (Sigma Aldrich, Berlin, Germany) and distilled water.

For the production of scaffolds, we used the foam replication method adapted from S. Kunjalukkal Padmanabhan et al. [11], starting from polyvinyl alcohol 4% (PVA) (Sigma Aldrich, Berlin, Germany), Triton X-100 surfactant (Sigma Aldrich, Berlin, Germany), polyurethane sponges (density of 23 kg/m<sup>3</sup>, provided by Fleximob, Constanța, Romania) and distilled water.

## 2.2. Methods

### 2.2.1. Synthesis of Hap/WS Composite Ceramic Powders

Considering the method described by R. Morsy et al. [13], Hap was obtained (maintaining the Ca/P molar ratio at 1.67) in the first step by dropping an H<sub>3</sub>PO<sub>4</sub> solution over the Ca(OH)<sub>2</sub> suspension, with a drop rate of 0.03 mL/s, at 80 °C, thus obtaining a precipitate through continuous magnetic stirring. In the second stage, Ca(NO<sub>3</sub>)<sub>2</sub> 4H<sub>2</sub>O was added over the precipitate, under magnetic stirring and maintaining the temperature, until its complete dissolution was achieved. Na<sub>2</sub>SiO<sub>3</sub> 9H<sub>2</sub>O was added dropwise over the precipitate, under the same conditions, maintaining a Ca/Si molar ratio of 1, in order to obtain the wollastonite phase. The pH of the final precipitate was adjusted between 10 and 10.5 by adding NH<sub>3</sub>, and the precipitate was left under magnetic stirring for 2 h at 80 °C, then kept for aging for 24 h. The precipitate was washed with distilled water, then filtered and dried in an oven at 80 °C for 24 h. After drying and grinding, a thermal treatment (calcination) was applied, leading to the formation of the composite powders. The temperature increase was carried out at 10 °C/min and was maintained for 2 h at 1000 °C. Studies have shown that this temperature is optimal for the formation of both the hydroxyapatite and the wollastonite phases [15–19]. The weight ratios of the composite Hap/WS powders are 90/10, 70/30, 50/50, 30/70 and 10/90 (Table 1). Also, simple powders of hydroxyapatite (Hap) and wollastonite (WS) were obtained through the same synthesis route. The powders were characterized using X-ray diffraction (XRD: XRD 6000 equipment, Shimadzu, Kyoto, Japan). The stages used to obtain the ceramic powders are presented in Figure 1.

**Table 1.** Composition of synthesized ceramic powders.

Hydroxyapatite/Wollastonite Mass Ratio (wt %)	Sample Code
90/10	9 Hap/1 WS
70/30	7 Hap/3 WS
50/50	5 Hap/5 WS
30/70	3 Hap/7 WS
10/90	1 Hap/9 WS

### 2.2.2. Synthesis of the Scaffolds

For the production of scaffolds (Figure 2), we adapted the method presented by S. Kunjalukkal Padmanabhan et al. [11]. The dispersion solution used for the formation of the suspensions was obtained by homogenizing PVA in distilled water, at 80 °C, under magnetic stirring. The PVA solution was magnetically stirred, and 0.8% Triton X-100 surfactant was added until its homogenization. The ceramic powders previously prepared were gradually added over the dispersion medium, in a ratio of 2:1, thus obtaining the ceramic suspension into which the polyurethane sponges, with dimensions of 1 × 1 × 1 cm, were immersed. The impregnation of the sponges was carried out using compression with a glass rod to remove the air, immersion in the ceramic suspension and removal of the compression force (of the glass rod); these operations were repeated 5 times. The sponges were squeezed to remove the excess suspension and dried at room temperature for 24 h, then heat treated to 400 °C at a ramp rate of 1 °/min; this temperature was maintained for 3 h to facilitate the burnout of the polyurethane sponge (according to the thermal analysis performed on the polyurethane sponge). Then, the probes were sintered at 1200 °C, with an increase rate of 5 °C/min for 3 h. The sintering temperature of 1200 °C was selected to keep

the polymorphic form of  $\beta$ -wollastonite in the material structure. According to the phase diagram for the binary CaO–SiO<sub>2</sub> system, above a temperature of 1124 °C, it begins to pass into the high-temperature  $\alpha$ -wollastonite form [8,10]. Then, the obtained scaffolds were characterized using scanning electron microscopy (SEM), bioactivity testing in a simulated physiological fluid environment, and also using biological tests regarding cell viability.

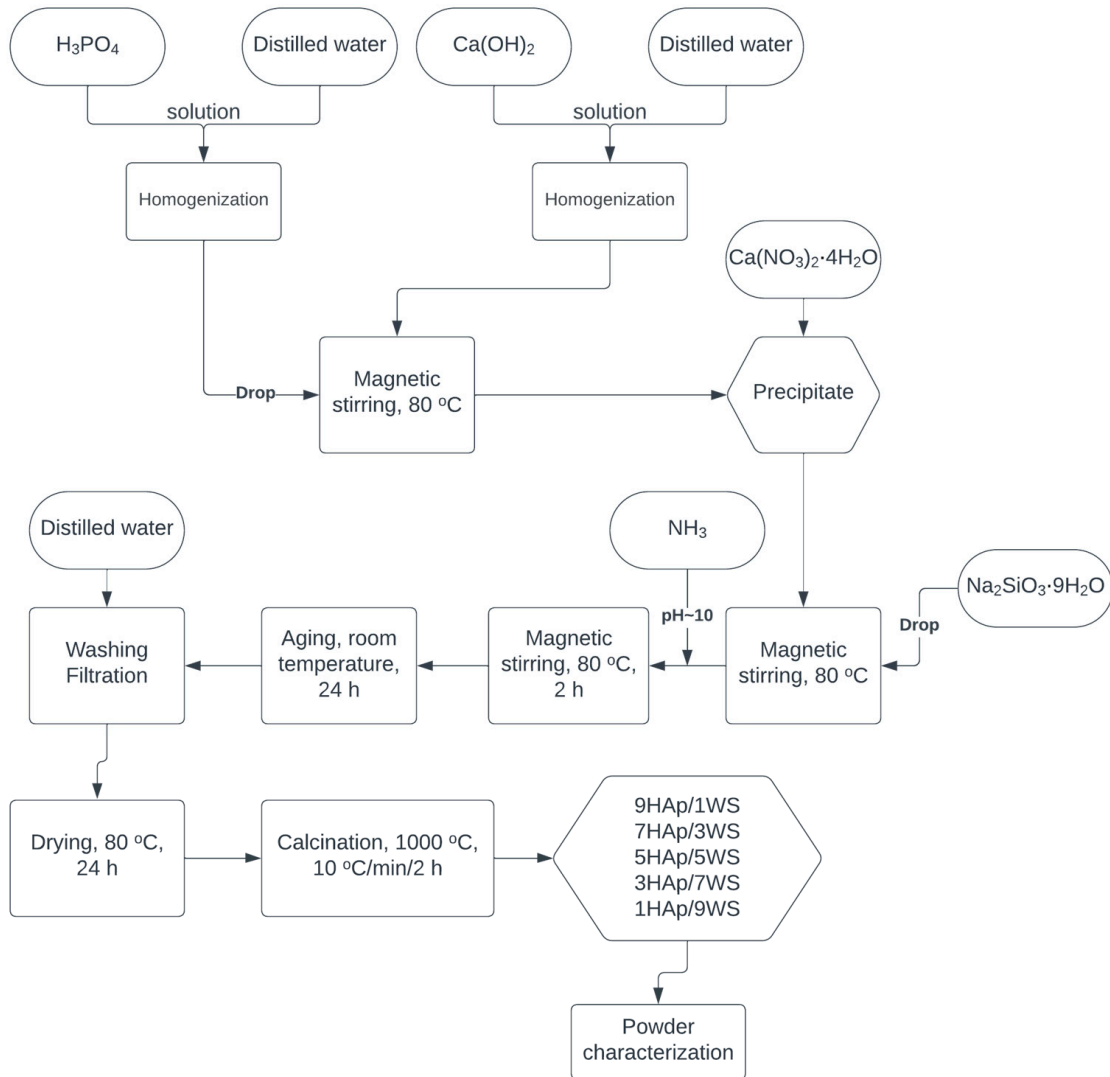


**Figure 1.** Schematic representation of the obtained ceramic powders with different weight ratios.

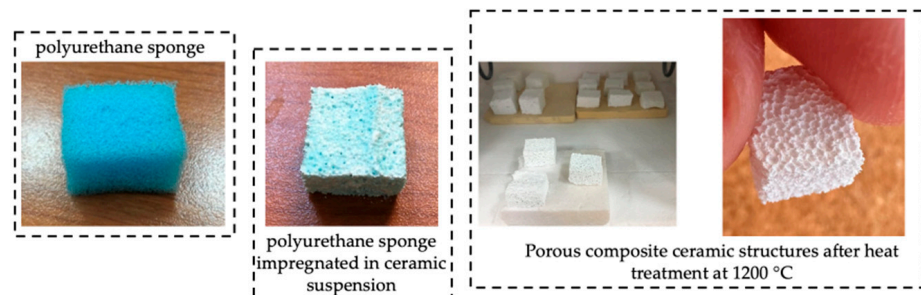


**Figure 2.** Schematic representations of the polyurethane sponge, sponge immersed in ceramic suspension and porous ceramic structures after thermal treatment at a temperature of 1200 °C.

### 2.3. Characterization Techniques

#### 2.3.1. Characterization of Hap/WS Composite Powders

The crystalline phases and the degree of crystallinity of the powders were evaluated via X-ray, at room temperature. The incident radiation used from the X-ray tube was Cu K $\alpha$  type ( $\alpha = 1.5406 \text{ \AA}$ ). The samples, previously grounded to obtain a very fine powder, were scanned at Bragg angle ( $2\theta$ ) values between  $20$  and  $80^\circ$ , with a scan step of  $0.02^\circ$  and a counting time of  $0.6 \text{ s/step}$ . The average crystallite size specific to each phase identified in each sample was calculated using the Debye–Scherrer Formula (1):

$$D = \frac{k\lambda}{\beta \cos\theta} \quad (1)$$

where  $D$  is the crystallite size ( $\text{\AA}$ ),  $k$  is a dimensionless factor with a value of  $0.9$ ,  $\lambda$  is the specific X-ray wavelength ( $1.5406 \text{ \AA}$ ),  $\beta$  is the width at half height (rad) and  $\theta$  is the Bragg angle (rad).

#### 2.3.2. Characterization of the Commercial Polyurethane Sponge

##### Thermal Analysis (DTA-TG)

The thermal analysis (DTA-TG) was performed using a Shimadzu DTG-TA-51H equipment (Shimadzu, Kyoto, Japan), in the  $20$ – $1000^\circ\text{C}$  temperature range, with a heating rate of  $10^\circ\text{C/min}$  in air, using the platinum crucible.

#### 2.3.3. Characterization of Hap/WS Composite Scaffolds

##### Morphology of Scaffolds

The microstructure, morphology and particle sizes, as well as the homogeneity between the 2 ceramic phases, were observed with scanning electron microscopy (SEM: HITACHI S2600N equipment, Tokyo, Japan). To facilitate the acquisition of virtual images, the samples were covered with a thin golden metallic layer.

##### Mechanical Properties

The mechanical compressive strengths of ceramic scaffolds with different Hap:WS mass ratios, with dimensions of  $1 \times 1 \times 1 \text{ cm}$ , sintered at  $1200^\circ\text{C}$  for  $3 \text{ h}$ , were determined using a testing machine (Shimadzu Autograph type AGS-X 20 kN equipment, Shimadzu, Kyoto, Japan). A speed of  $0.5 \text{ mm/min}$  was used for the determination. Three samples of each type were tested in order to obtain the mechanical compressive strength. The use of three samples aligns with testing standards (ASTM International) [20], which often recommend a minimum of three samples for reliable results. A number of three samples is often used in the field and is widely accepted for similar materials, providing a balance between practicality and statistical significance.

##### Bioactivity of the Scaffolds in Simulated Body Fluid (SBF)

The bioactivity of the samples was determined after immersion in simulated body fluid, prepared according to the protocol described by T. Kokubo et al. [21], for  $21$  days, in order to observe the microstructure. Scaffolds of each type of Hap/WS mass ratio were introduced into a cell culture plate, and the microstructures were observed for  $21$  days, at a temperature of  $37^\circ\text{C}$ , in a water bath (BAE-6 equipment, Raypa, Barcelona, Spain).

##### Biocompatibility Assessment

The cell viability tests were carried out at Horia Hulubei National Institute for R&D in Physics and Nuclear Engineering on MG-63 osteoblast-like cells (CLS, Heidelberg, Germany) cultured in DMEM culture medium (PAN-Biotech, Aidenbach, Germany) supplemented with  $10\%$  fetal bovine serum (FBS) and  $1\%$  penicillin, under standard conditions of temperature and humidity ( $37 \pm 2^\circ\text{C}$ ,  $5 \pm 1\% \text{ CO}_2$ , humidity greater than  $90\%$ ).

The hydroxyapatite and wollastonite porous structures were sampled following the guidelines from ISO 10993-12:2021 [22]. Then, the samples were sterilized using gamma ionizing radiation ( $\text{Co}^{60}$ ), using a radiator (SVST Co-60/B type radiator, Institute of Isotopes Co. Ltd., Budapest, Hungary) for 14 h and 45 min, with an absorbed dose in the following range (determined with a confidence level of 95%):  $D_{\text{min}} = 28.6 \pm 1.7$  kGy;  $D_{\text{max}} = 40 \pm 2.1$  kGy.

The viability of cells in contact with the hydroxyapatite and wollastonite porous structures was assessed using the MTS tetrazolium salt assay, according to ISO 10993-5:2009 [23]. Ceramic samples were introduced under sterile conditions into a cell culture plate, and 100,000 cells/500  $\mu\text{L}$  complete culture media were seeded onto each scaffold. The samples were incubated for 1 h to allow cells to adhere; then, culture medium was added over the samples to completely immerse the ceramic structures. The work plates were incubated under standard conditions of temperature and humidity for 7 days. After this period, 20% MTS solution of the total medium volume was added to each well, and the samples were incubated for another 2 h. The last step in the process of evaluating the biological effect of the samples was to add 100  $\mu\text{L}$  of the resulting solution to a new plate and read the absorbances on a spectrophotometer (Mithras LB 940 equipment, Berthold Technologies, Bad Wildbad, Germany) at a wavelength of 490 nm.

In order to qualitatively evaluate the morphology of the cells in contact with the porous ceramic structures, scanning electron microscopy evaluation was employed following incubation of the samples with osteoblast-like cells for 7 days. The samples were sterilized with gamma ionizing radiation ( $\text{Co}^{60}$ ), using a radiator (SVST Co-60/B type radiator, Institute of Isotopes Co. Ltd., Budapest, Hungary) for 14 h and 45 min, with an absorbed dose contained in the following range (determined with a confidence level of 95%):  $D_{\text{min}} = 28.6 \pm 1.7$  kGy;  $D_{\text{max}} = 40 \pm 2.1$  kGy. MG63 osteoblast cells were cultured in DMEM culture medium (PAN-Biotech, Aidenbach, Germany) supplemented with 10% fetal bovine serum (FBS) and 1% penicillin. Ceramic samples were introduced, under sterile conditions, into a 12-well plate, adding 100,000 cells/well to the surface of each scaffold. Culture medium was added over the samples to completely cover them. The work plate was incubated under standard conditions of temperature and humidity ( $37 \pm 2$  °C,  $5 \pm 1\%$   $\text{CO}_2$ , humidity greater than 90%) for 7 days. After this period, the culture medium was removed, and the samples were washed with PBS and fixed with 2.5% glutaraldehyde solution in PBS for 1 h at 37 °C. The samples were washed again with PBS and dehydrated in 3 steps for 30 min each with 70%, 90% and 100% EtOH. Finally, the samples were also dehydrated with HMDS:EtOH 50:50, 25:75 and 0:100 for 6 min for each ratio and dried for 24 h at room temperature. The scanning electron microscopy (SEM) technique was used to qualitatively evaluate the cell morphology (SEM: HITACHI S2600N equipment, Tokyo, Japan). The investigations were conducted following the sectioning of the material, in order to evaluate the volume of the samples.

All experiments were performed in triplicate for each type of ceramic scaffold. Cell viability was calculated relatively to the negative control, which was attributed a value of 100% viability. Data are expressed as mean  $\pm$  standard deviation (STDEV), and statistical evaluation was performed using Student's *t*-test.

### 3. Results and Discussion

Figure 3 shows the diffractograms of the composite ceramic powders, with different Hap/WS mass ratios, thermally treated at a temperature of 1000 °C for 2 h. The mineralogical phases identified are hydroxyapatite and  $\beta$ -wollastonite, according to JCPDS numbers 072-1243 and 99-101-2916, respectively. Hydroxyapatite crystallized in the hexagonal system, and the cell parameters are  $a = b = 9.432$  Å and  $c = 6.881$  Å.  $\beta$ -wollastonite crystallized in the triclinic system, and the cell parameters are  $a = 7.94$  Å,  $b = 7.32$  Å,  $c = 7.07$  Å,  $\alpha = 90.03$  °,  $\beta = 95.37$  °,  $\gamma = 103.43$  °. Both hydroxyapatite and wollastonite show a high degree of crystallinity characterized by the presence of diffraction maxima (diffraction interference) of high intensity. It was also observed that by increasing the content of

wollastonite in the composition of the analyzed powders, the maximum intensity of the diffraction specific to the WS phase increases, compared to the diffraction interferences specific to the Hap phase, which show a diffraction maximum in the 9 Hap/1 WS sample, this being observed more closely in Figure 3b. Table 2 shows the average crystallite sizes obtained by applying the Debye–Scherrer calculation formula. The data show that the average crystallite sizes for the five types of powders obtained are of nanometric order, and the differences between them are insignificant. The literature [24] suggests that compared to the morphology and composition of human bone, the crystallite size of hydroxyapatite (a nanometer size) and the morphology obtained by wet synthesis (precipitation) are similar to those of human bone, despite the fact that it can have different properties and characteristics, or it can be used in a mixture with an organic or inorganic phase (as described in the present study). These features are essential in ion exchange and substitution, thus playing a vital role in osteogenesis and angiogenesis, feasible for natural bone formation. Also, the specialized literature [25] suggests that both smaller crystallite and granule sizes, of nanometric order, generally increase the degree of biodegradation. We can state, according to the presented results, that composite powders based on hydroxyapatite and wollastonite were successfully obtained by the in situ method.

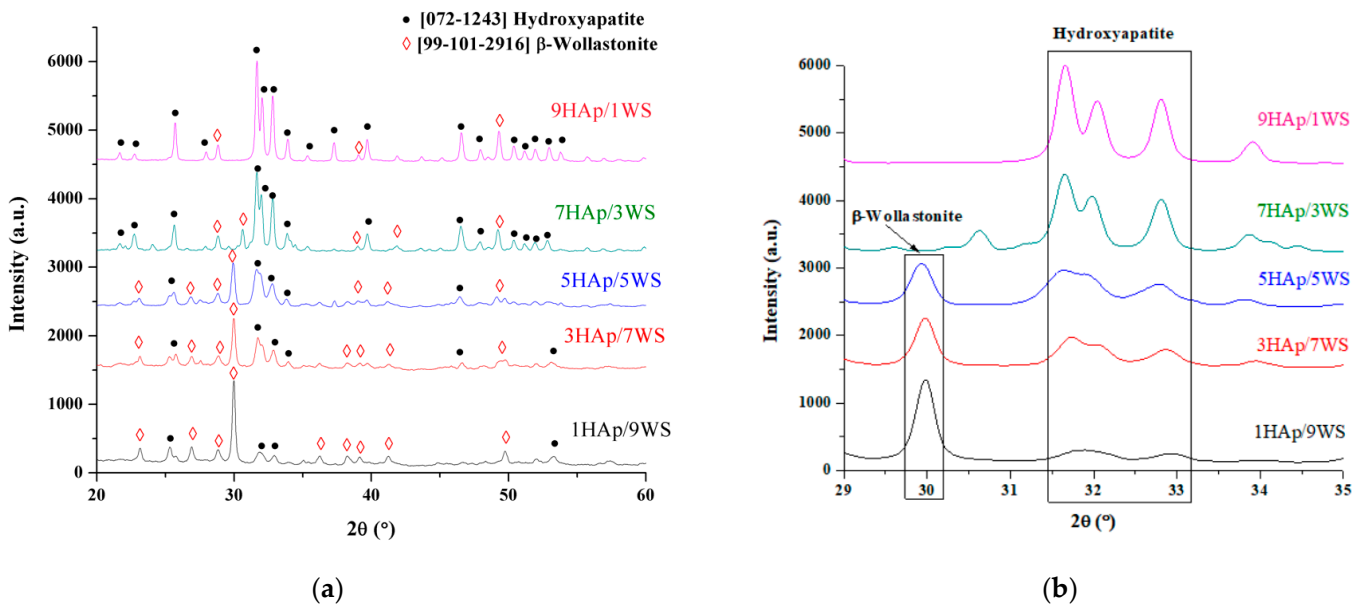


**Figure 3.** (a) X-ray diffractograms recorded for the composite ceramic powders, with different mass ratios Hap/WS, thermally treated at a temperature of 1000 °C and (b) zoom made on region 2θ:29–35.

**Table 2.** Average crystallite sizes of Hap/WS powders treated at a temperature of 1000 °C.

Sample	Crystallite Size (nm)	
	Hap	WS
9 Hap/1 WS	7.10 ± 0.42	7.37 ± 0.83
7 Hap/3 WS	5.81 ± 1.00	5.75 ± 1.13
5 Hap/5 WS	4.53 ± 1.65	4.28 ± 0.48
3 Hap/7 WS	4.28 ± 0.64	4.69 ± 0.69
1 Hap/9 WS	4.54 ± 1.12	4.71 ± 0.65

The thermal analysis (Figure 4) performed on the polyurethane sponge indicated three exothermic effects on the DTA curve, with their maxima at 300.97 °C, 336.85 °C, and 493.19 °C, respectively. Effects were caused by the combustion of the organic component. It can also be noticed, according to the TGA curve, that in the temperature range 30–400 °C, the mass loss values are above 90%. Thus, according to these data, we selected

the first temperature on the heat treatment curve of porous structures, 400 °C. According to literature studies, the polyurethane sponge, especially the commercial one, is a polymer that can contain other additives. Thus, during the heat treatment, this causes pyrolysis and combustion reactions. During the pyrolysis process (between 200 °C and 300 °C), the formed groups break down into isocyanates and polyols. Between 300 °C and 500 °C the residues decompose into amines, ethers and CO<sub>2</sub>. At temperatures greater than 600 °C, polyols fragment and volatilize and, as the temperature increases, carbon results that can further decompose, leaving behind a residue at temperatures greater than 800 °C [26,27].

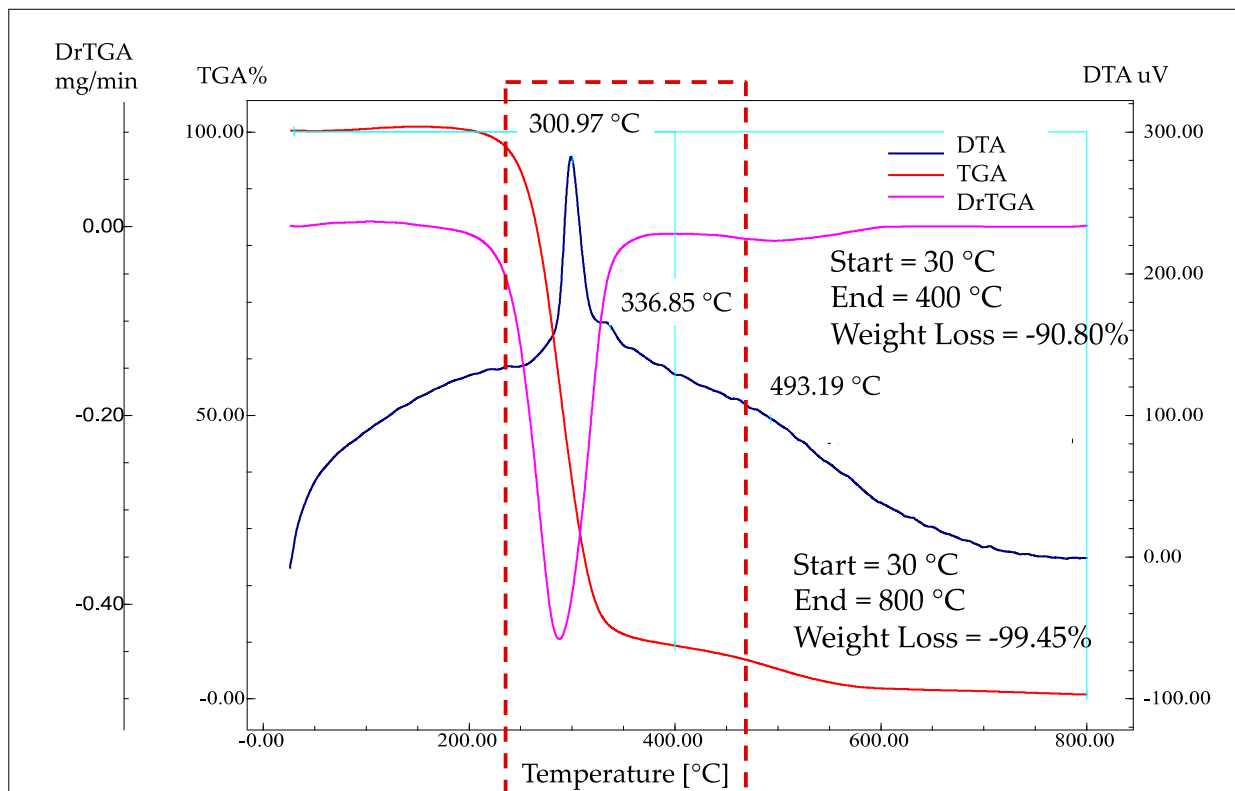


**Figure 4.** Derivatogram of the polyurethane sponge.

SEM images show the microstructure of the scaffolds with different mass ratios between the two phases (Figure 5). All three-dimensional structures show an open porosity and a high volume of interconnected pores, with an average size of approximately 300  $\mu\text{m}$ , regardless of the composition of the analyzed scaffolds (Table 3). According to the data presented in Table 3, it can also be observed that, by increasing the WS content, there is a slight increase in the minimum value of porosity. The distribution of the pores is varied, falling within the optimal range that facilitates the processes of osteogenesis and angiogenesis (100–700  $\mu\text{m}$ ) [28], as well as the diffusion of oxygen and nutrients and the attachment and proliferation of cells. The SEM images shown in Figure 5G–L show the microstructure of the 5 Hap/5 WS sample, the irregular and acicular morphology of some platelet-type particles and a morphology specific to the wollastonite phase distributed among quasi-spherical particles that can be associated with hydroxyapatite. Thus, the two ceramic phases present in the composition of the sample can be identified. As the mass ratio between Hap and WS increases, the particles show a much more spherical morphology. The specific morphology of wollastonite particles, respectively those of hydroxyapatite, were also highlighted by S. Kunjalukkal Padmanabhan et al. [11] and Kaili Lin et al. [14]. Also, according to the data presented in Table 3, it can also be noticed that, by increasing the WS content, there is a slight increase in the minimum value of porosity, which may be due to the acicular morphology of the WS particles, also stated by Kaili Lin et al. [14]. In Figure 5J–L,

the high sintering capacity of the spherical Hap particles can be observed, resulting in a well-defined structure. Also, all of the microstructures have bridges containing pores with nanometric dimensions, the sample 7 Hap/3 WS having internal pores with dimensions between 52.81 and 693.1 nm.

**Table 3.** The pore sizes associated with each microstructure.

Sample	Pore Size ( $\mu\text{m}$ )
9 HAp/1 WS	107.48–628.2
7 HAp/3 WS	113.7–615.38
5 HAp/5 WS	123.08–621.54
3 HAp/7 WS	123.85–615.38
1 HAp/9 WS	112.3–612.46

The effect of the HAp/WS mass ratio on the mechanical compressive strength can be seen in Table 4. The HAP control sample has a compressive strength value of  $0.25 \pm 0.05$  MPa, while the WS control sample indicates a value of  $0.10 \pm 0.06$  MPa, thus demonstrating the low mechanical strength of calcium silicate. By comparison with the values obtained by S. Kunjalukkal Padmanabhan et al. on the plain HAp and WS samples, the results are not significantly different, with slightly higher values of  $0.51 \pm 0.14$  MPa for HAp and  $0.21 \pm 0.1$  MPa for WS, respectively [11]. Also, Gurbinder Kaur et al. mention in their study that for WS obtained by the same technique of replicating a polyurethane sponge, the mechanical resistance to compression can have values between 0.4 MPa and 3.6 MPa [29]. According to the stated data, the presence of wollastonite in the composition of the ceramic structures initially shows an increase in the mechanical resistance to compression, obtaining values of  $1.14 \pm 0.21$  MPa and  $0.90 \pm 0.10$  MPa for the 9 HAp/1 WS and 7 HAp/3 WS samples, respectively; these value fall within the range of 0.2–4 MPa, specific to the mechanical resistance to compression of trabecular bone with a porosity of 90% [30]. However, a further increase in the WS content of the ratio (5 HAp/5 WS, 3 HAp/7 WS and 1 HAp/9 WS) results in a decrease in the mechanical compressive strength ( $0.41 \pm 0.12$  MPa,  $0.21 \pm 0.13$  MPa and  $0.17 \pm 0.14$  MPa, respectively), which is also confirmed in previous studies [2,11,29]. Also, Sanosh Kunjalukkal Padmanabhan et al., in their study published in 2011, obtained porous structures based on HAp/WS with techniques similar to those presented in this study, where for a ratio of 50:50 HAp:WS they obtained a mechanical resistance to compression of 1.2 MPa, and for porous structures based on HAp, values of mechanical resistance to compression of 0.6 MPa. The porous ceramic bodies were sintered at a temperature of 1300 °C, and according to the diffractograms, a mixture of phases of  $\alpha$ -wollastonite, hydroxyapatite and  $\beta$ -tricalcium phosphate was obtained [31]. Thus, it can be stated that, in order to increase the mechanical resistance of hydroxyapatite, which has a brittle character, this material can be “reinforced” with another phase that limits this effect. Wollastonite, due to the morphology of its particles and its ability to prevent the formation of defects in the microstructure, increases the value of the mechanical compressive strength of hydroxyapatite when the ratio is a maximum 30%. Literature studies [11] suggest that the mechanical properties of porous structures are influenced by morphology, porosity and grain size; furthermore, wollastonite presents an acicular particle morphology, which makes it a good candidate for use as a reinforcement material, thus improving the mechanical resistances for porous structures based on calcium silicate.

In the present study, as mentioned, wollastonite improves the mechanical compressive strengths for the porous samples where it is used at a maximum percentage of 30%. Above this value, the studied properties decrease, which may be due to abnormal growth of the wollastonite grains; if the proportion of hydroxyapatite is not sufficient, the acicular grains of the wollastonite cannot properly reinforce the material, and the pores of the material thereby present bridges with micropores and also lead to an improper sintering structure. According to the SEM images shown in Figure 5J–O, the 9 HAp/1 WS and

7 HAp/3 WS samples present well-defined structures, in which the wollastonite particles are embedded between the hydroxyapatite ones, a phenomenon that determined the increase in mechanical strength.

The morpho-structural changes of the five ceramic samples with different HAp/WS mass ratios after 21 days in SBF can be seen in the SEM images in Figure 6. All of the scaffolds show high mineralization in the simulated physiological serum, as evidenced by the presence of new mineralization nuclei, specific to the formation of a new layer of carbonated calcium phosphates on the surface, compared to the SEM images of the samples before immersion in SBF. Literature studies suggest that on the surface of such materials, there is a rapid exchange of  $\text{Na}^+$  and  $\text{Ca}^{2+}$  ions with  $\text{H}^+$  and  $\text{HO}^-$  ions from the solution, leading to the hydrolysis of silica groups, with the formation of silanol groups (Si-OH). Cation exchange increases the concentration of hydroxyl ions in the solution, which leads to an attack on the silica network. Silica passes into the solution in the form of  $\text{Si}(\text{OH})_4$ , resulting from the breaking of the Si-O-Si bonds, followed by the continuous formation of Si-OH (silanols) at the interface. Subsequently, the condensation and repolymerization of a layer rich in  $\text{SiO}_2$  takes place on the surface material that is depleted (deficient) of alkaline and alkaline earth cations. Then, the migration of  $\text{Ca}^{2+}$  and  $\text{PO}_4^{3-}$  ions to the surface through the layer rich in  $\text{SiO}_2$  takes place, forming above it a film that is rich in  $\text{CaO-P}_2\text{O}_5$  and amorphous, which grows by incorporating calcium and phosphates from the solution; this ultimately leads to the crystallization of the amorphous film rich in  $\text{CaO-P}_2\text{O}_5$  by incorporating  $\text{OH}^-$  and  $\text{CO}_3^{2-}$  anions from the solution, with the formation of a mixed layer containing carbonated hydroxyapatite (HCA) [32–34].

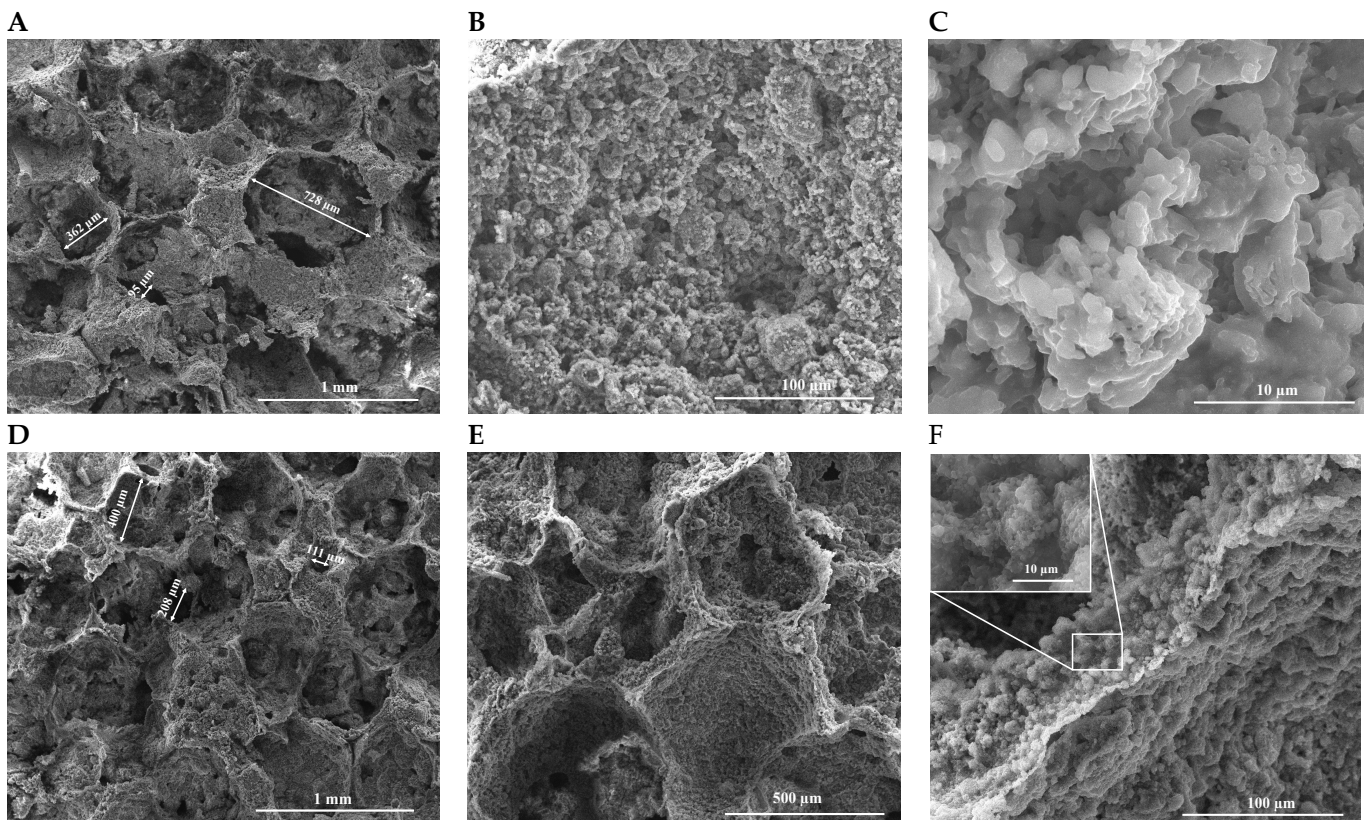
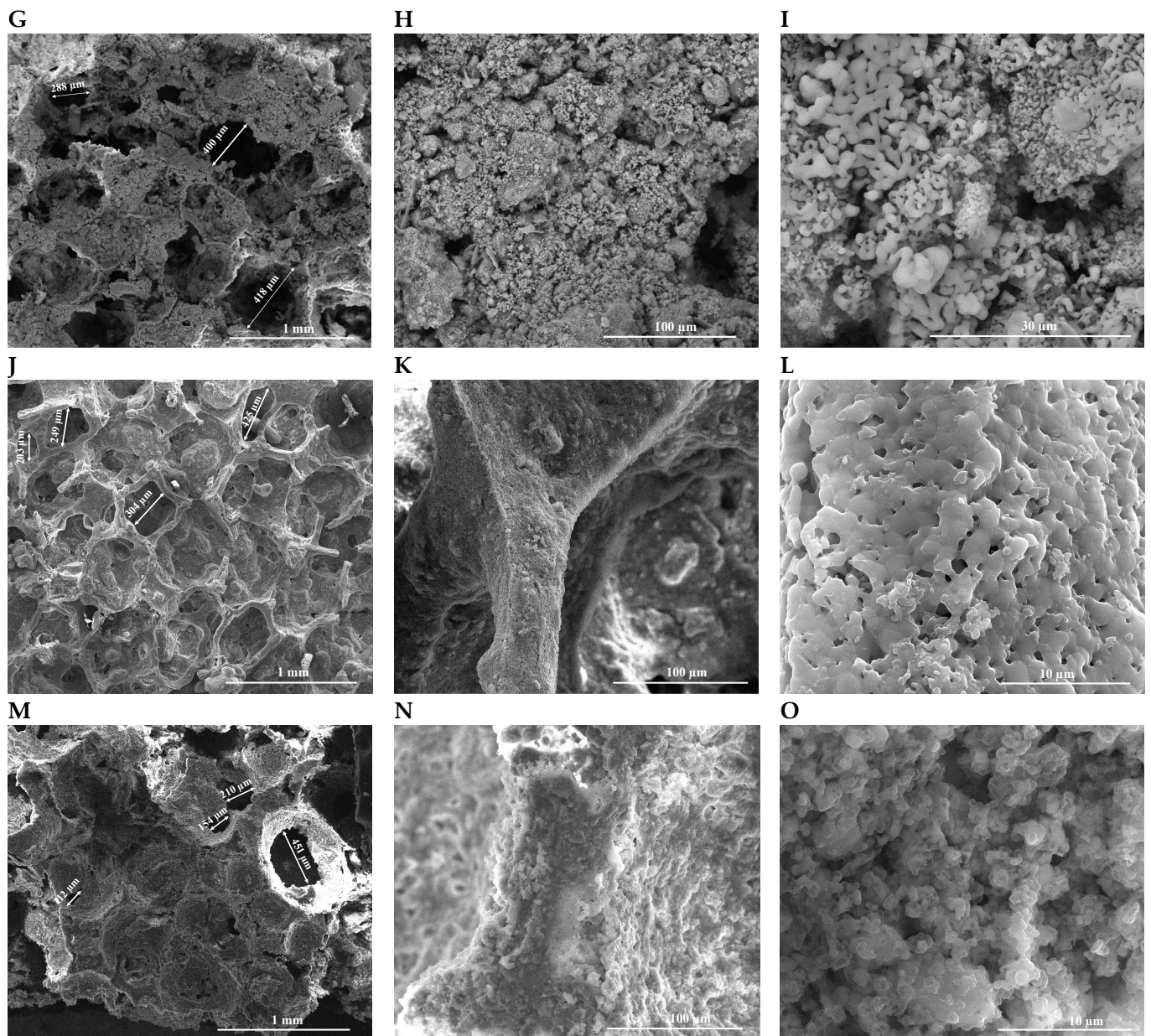


Figure 5. Cont.



**Figure 5.** SEM images of porous structures: (A–C) 1 Hap/9 WS, (D–F) 3 Hap/7 WS, (G–I) 5 Hap/5 WS, (J–L) 7 Hap/3 WS and (M–O) 9 Hap/1 WS, at magnifications of 100 $\times$ , 1000 $\times$ , and 10,000 $\times$ , respectively.

**Table 4.** Mechanical compressive strength values of porous ceramic structures.

Sample	Mechanical Compressive Strength (MPa)
HAp	0.25 $\pm$ 0.05
9 HAp/1 WS	1.14 $\pm$ 0.21
7 HAp/3 WS	0.90 $\pm$ 0.10
5 HAp/5 WS	0.41 $\pm$ 0.12
3 HAp/7 WS	0.21 $\pm$ 0.13
1 HAp/9 WS	0.17 $\pm$ 0.14
WS	0.10 $\pm$ 0.06

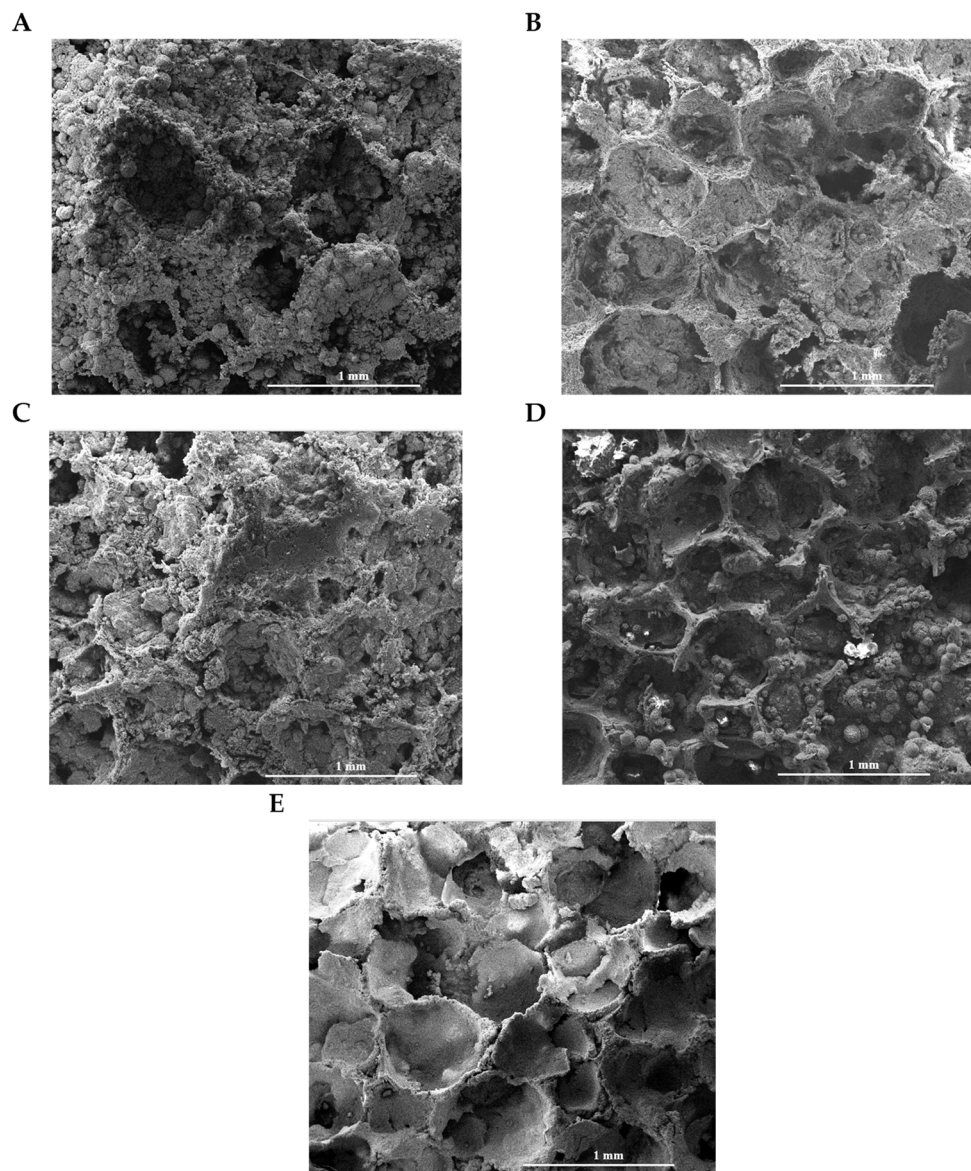


**Figure 6.** SEM images of porous structures: (A) 1 HAp/9 WS, (B) 3 HAp/7 WS, (C) 5 HAp/5 WS, (D) 7 HAp/3 WS and (E) 9 HAp/1 WS after 21 days in SBF.

Analyzing the microscopy images in Figure 6, it can easily be observed in the SEM micrographs that a much more pronounced mineralized surface is present in the case of the samples with a higher content of wollastonite in the composition, aspects reported by Kaili Lin et al. [14].

The interaction of HAp/WS samples with osteoblast-like cells was assessed following 7 days of incubation, which is a suitable timepoint to have a clear picture of the ability of the ceramic porous samples to sustain the attachment and growth of the cells.

The quantitative viability assessment of the osteoblast-like cells cultured on the ceramic samples was carried out using the MTS tetrazolium salt viability assay, which provides a direct measure of the cells' metabolism. For this, cell viability was expressed as a percentage of the negative control (where the viability of the negative control was established to be 100%).

According to Figure 7, the highest cell viabilities were recorded for the samples with a higher content of hydroxyapatite, for which the 9 HAp/1 WS sample presented a cell viability of  $100.04 \pm 0.99\%$  and the 7 HAp/3 WS sample presented a cell viability of  $103.11 \pm 0.47\%$  compared to the control sample (not significant—NS). By increasing the

WS content, a slight decrease in the cell metabolism was noticed, as the values for the cell viability decreased to  $75.22 \pm 0.06\%$  (NS),  $70.14 \pm 0.01\%$  ( $p = 0.01$ ) and  $70.48 \pm 0.03\%$  ( $p = 0.02$ ) compared to the control for the 5 HAp/5 WS, 3 HAp/7 WS and 1 HAp/9 WS samples, respectively. It can be noticed that a higher content of hydroxyapatite constitutes a more favorable environment for cell viability, due to the biomimetic composition of the material. The decrease in cell viability is attributed to the presence of wollastonite in the composition of the ceramics, and the trend is proportional to the wollastonite concentration increase (significant compared to the negative control). This means that higher concentrations of wollastonite affect the metabolism of the osteoblast-like cells. The slight decrease in viability for samples with higher wollastonite content can also be attributed to the platelet and acicular morphology of the particles, which may hinder the process of cell attachment compared to the quasi-spherical morphology of the hydroxyapatite particles. However, all of the samples show high biocompatibility, exceeding the standard value of 70% imposed by the ISO 10993-5:2009 standard [23]; thus, they are capable of being used in tissue engineering applications of bone tissue.

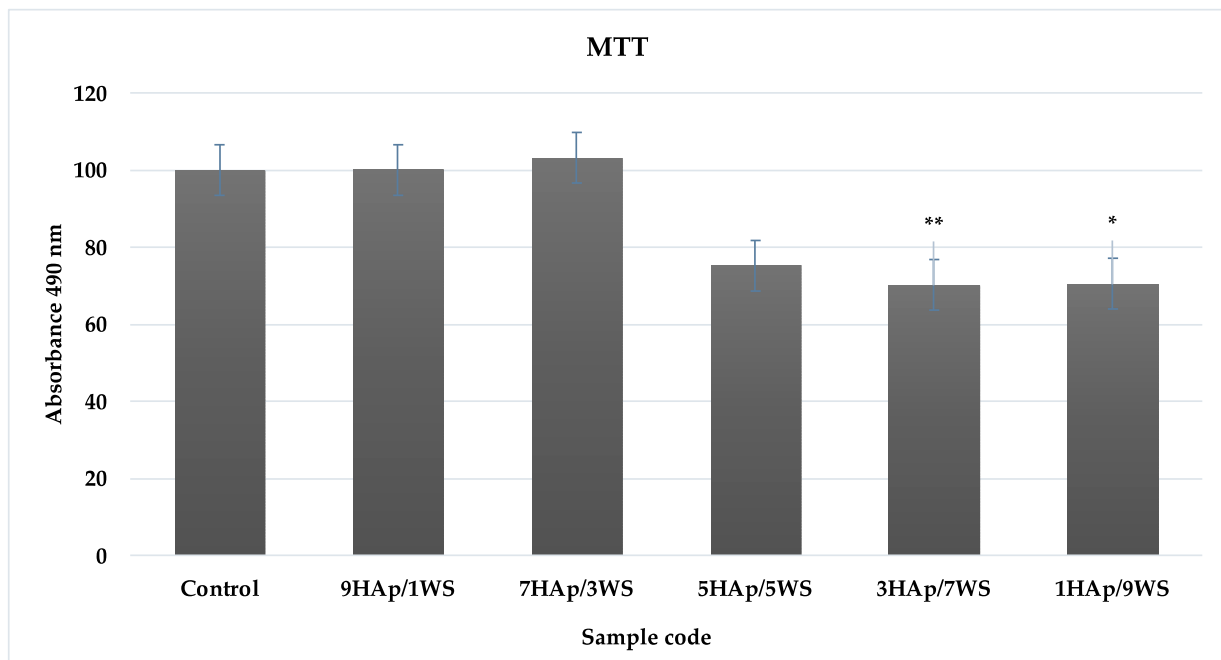


**Figure 7.** Cell viability profile of MG-63 osteoblast-like cells following 7 days of incubation on HAp/WS scaffolds. Results are represented as mean  $\pm$  STDEV ( $n = 3$ ); statistical significance: \*  $p < 0.05$ , \*\*  $p < 0.01$ .

The scanning electron microscopy (SEM) technique was used for the qualitative evaluation of cell morphology in the volume of the HAp/WS samples, using a HITACHI S2600N type of equipment. The specific SEM micrographs of cells following 7 days of incubation on the ceramic samples are shown in Figure 8. Given the dimension of the HAp/WS samples used in this investigation, as well as the 3D porous architecture, it is difficult to perform a quantitative assessment of the cells. However, the investigation was carried out in the volume of the HAp/WS samples to emphasize the ability of the cells to penetrate the ceramic samples' structures. The high attachment capacity of osteoblast-type cells was observed on the surface of all of the synthesized materials. The cells have a flattened morphology, which is specific to a good attachment process [35–38]. Also, a flattened morphology is a direct indicator of a viable cell adhering to a biocompatible substrate [35–38], whilst a round-shaped morphology indicates weak attachment of cells or even cell death [39]. Moreover, due to the 3D environment given by the architecture of the porous HAp/WS ceramics, the osteoblasts exhibit numerous ramifications that

strengthen their interaction with the ceramic substrate, providing many attachment points for the cells. The architecture of the materials enables a biomimetic morphology of the osteoblast cells that is similar to their natural environment. Finally, these data can also be correlated with the information recorded by the MTS test (Figure 7), which demonstrate good biocompatibility of the porous ceramic structures.

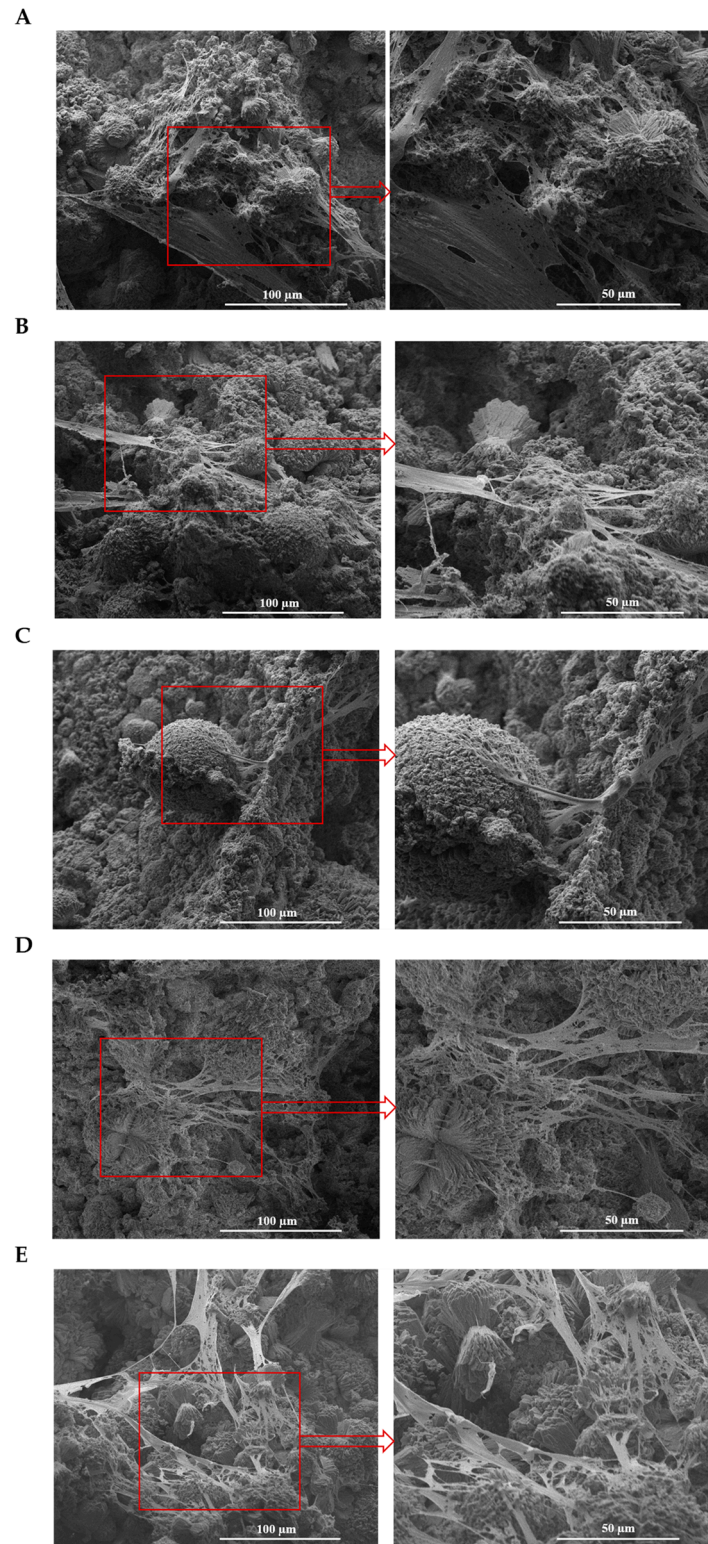


**Figure 8.** SEM micrographs of porous structures with osteoblast-like cells on (A) 1 HAp/9 WS, (B) 3 HAp/7 WS, (C) 5 HAp/5 WS, (D) 7 HAp/3 WS and (E) 9 HAp/1 WS after 7 days.

The HAp/WS ceramic porous samples provide a biocompatible substrate for cells to adhere to and to grow upon, as shown through the viability investigations and morphological assessment of osteoblast-like cells cultured for 7 days on the ceramic scaffolds. Additionally, the bioactive character of the samples that was proven through in vitro testing shows the potential use of these materials in tissue engineering of bone applications.

#### 4. Conclusions

The aim of this study was to obtain and investigate porous composite ceramic structures based on hydroxyapatite and wollastonite. In the first stage, ceramic powders were synthesized using a coprecipitation method with different mass ratios between the two phases (9 HAp/1 WS, 7 HAp/3 WS, 5 HAp/5 WS, 3 HAp/7 WS and 1 HAp/9 WS). The mineralogical composition of the composite powders was analyzed using X-ray diffraction, which showed the formation of two phases, hydroxyapatite and wollastonite. Later, the composite powders were used to obtain porous structures. These structures were obtained using the method of replicating a polyurethane sponge and applying an appropriate heat treatment; for the burning of the sponge, according to the thermal analysis, a temperature of 400 °C was applied for 3 h, and for the consolidation of the ceramic structure, a temperature of 1200 °C was selected. The porous structures were investigated, and from a microstructural point of view, they presented a porous microstructure with interconnected pores, with a size varying between 100 and 700 µm according to the scanning electron microscopy images. The porous structures with hydroxyapatite mass contents of 90% and 70%, presented structures with a higher degree of densification, in which the wollastonite particles were homogenized into the hydroxyapatite mass. The mechanical properties of the porous structures are influenced by the degree of porosity, the size of the pores, the presence of pores in the connecting bridges, the granular size, etc. Thus, according to the results obtained from the mechanical compression resistance tests, the samples 9 HAp/1 WS and 7 HAp/3 WS presented the highest values of  $1.14 \pm 0.21$  and  $0.90 \pm 0.10$ , respectively, but these values decreased with the increase in WS content in the samples. The specialized literature suggests that wollastonite functions as a reinforcing material for structures based on hydroxyapatite, but only if it is added into composites to a maximum percentage of 50%. In the case of this study, the best mechanical resistance to compression was noticed for the samples that had a maximum percentage of 30% wollastonite in their composites; above this value, the mechanical properties to compression decrease, aspects that are influenced possibly by abnormal growth of the wollastonite grains, the impossibility of proper reinforcement of the material, the presence of larger pores in the connecting bridges and an increasingly smaller percentage of hydroxyapatite in the composites, which make the sintering process incomplete.

The bioactive characteristics of the samples were determined by immersing them in SBF for a period of 21 days. All of the porous structures showed high mineralization after 21 days due to the formation of an apatite layer on the surface, a process that is specific to the CaO–SiO<sub>2</sub> class of compounds. A much more pronounced mineralized surface was observed in the case of structures with a higher content of wollastonite in the composition, an aspect that was also suggested by the specialized literature.

The interaction of HAp/WS samples with osteoblast-like cells was evaluated after 7 days of incubation, and a quantitative evaluation of the viability of osteoblast-like cells cultured on the ceramic samples was determined using the MTS tetrazolium salt viability assay. The highest cell viabilities were recorded for the samples that had a higher hydroxyapatite content; thus, the 9 HAp/1 WS sample presented a cell viability of  $100.04 \pm 0.99\%$ , and the 7 HAp/3 WS sample presented a cell viability of  $103.11 \pm 0.47\%$ , compared to the control sample. At a wollastonite percentage greater than 30% in the composition of the structures, a decrease in cell viability was observed. This means that higher concentrations of wollastonite affect the metabolism of osteoblast-like cells. The slight decrease in viability for samples with higher wollastonite content can also

be attributed to the platelet and acicular morphology of the particles, which may hinder the cell attachment process compared to the quasi-spherical morphology of the hydroxyapatite particles.

Also, the high attachment capacity of osteoblast type cells can be observed in the SEM micrographs on the surfaces of all of the porous materials. The cells present a flattened morphology, which is typical of a good attachment process. The architecture of the obtained materials, which offers the cells an environment that is similar to their natural environment, has numerous ramifications that strengthen the interaction of the osteoblastic cells with the ceramic substrate, providing many attachment points for the cells.

We thereby conclude that by controlling the composition of such composite ceramic materials, promising materials can be obtained for their use in the field of bone tissue engineering. Also, an ideal composition can always be selected depending on the intended application and the structure to be reconstructed.

**Author Contributions:** Conceptualization, C.-D.G., G.V. and A.C.; methodology, C.-D.G. and A.C.; investigation, G.V., A.C., C.-A.B., V.D. and R.C.P.; writing—original draft preparation, A.C., C.-A.B., V.D. and R.C.P.; writing—review and editing, A.C., C.-A.B., V.D. and R.C.P.; visualization, C.-D.G. and G.V.; supervision, C.-D.G., G.V. and A.C.; resources, R.C.P. All authors have read and agreed to the published version of the manuscript.

**Funding:** The APC was funded by the National University of Science and Technology Politehnica Bucharest as a proof-of-concept project.

**Data Availability Statement:** The data presented in this study are available in article.

**Acknowledgments:** This research has been funded by the European Social Fund from the sectoral operational program Human Capital 2014–2020, through a financial agreement with the title “Training of PhD students and postdoctoral researchers in order to acquire applied research skills–SMART”, contract no. 13530/16.06.2022–SMIS code: 153734.

**Conflicts of Interest:** The authors declare no conflict of interest.

## References

1. Mohd, J.; Abid, H.; Ravi, P.S.; Rajiv, S. Sustaining the healthcare systems through the conceptual of biomedical engineering: A study with recent and future potentials. *Biomed. Technol.* **2023**, *1*, 39–47. [[CrossRef](#)]
2. Sharma, M.; Paul Khurana, S.M. *Omics Technologies and Bio-Engineering*; Biomedical Engineering; Academic Press: Cambridge, MA, USA, 2018; pp. 323–336. [[CrossRef](#)]
3. Baines, F.; Novajra, G.; Vitale-Brovarone, C. Bioceramics and Scaffolds: A Winning Combination for Tissue Engineering. *Front. Bioeng. Biotechnol.* **2015**, *3*, 202. [[CrossRef](#)] [[PubMed](#)]
4. Zafer, T.; Bretcanu, O.; Çaliskan, F.; Dalgarno, K. Fabrication of porous apatite-wollastonite glass ceramics using a two steps sintering process. *Mater. Today Commun.* **2022**, *30*, 103216. [[CrossRef](#)]
5. Zaman, S.U.; Irfan, M.; Irfan, M.; Muhammad, N.; Zaman, M.K.U.; Rahim, A.; Rehman, S.U. Overview of hydroxyapatite; composition, structure, synthesis methods and its biomedical uses. *Biomed. Lett.* **2020**, *6*, 84–99.
6. Haider, A.; Haider, S.; Han, S.S.; Kang, I.-K. Recent advances in the synthesis, functionalization and biomedical applications of hydroxyapatite: A review. *RSC Adv.* **2017**, *7*, 7442–7458. [[CrossRef](#)]
7. Ismail, H.; Mohamad, H. Bioactivity and biocompatibility properties of sustainable wollastonite bioceramics from rice husk ash/rice straw ash: A review. *Materials* **2021**, *14*, 5193. [[CrossRef](#)] [[PubMed](#)]
8. Imarally, V.; Nascimento, S.R.; Barbosa, W.T.; Carrodeguas, R.G.; Fook, M.V.L.; Rodríguez, M.A. Synthesis of Wollastonite Powders by Combustion Method: Role of Amount of Fuel. *Int. J. Chem. Eng.* **2018**, *2018*, 6213568. [[CrossRef](#)]
9. Milani, S.; Comboni, D.; Lotti, P.; Fumagalli, P.; Ziberna, L.; Maurice, J.; Hanfland, M.; Merlini, M. Crystal Structure Evolution of CaSiO<sub>3</sub> Polymorphs at Earth’s Mantle Pressures. *Minerals* **2021**, *11*, 652. [[CrossRef](#)]
10. Zenebe, C.G. A Review on the Role of Wollastonite Biomaterial in Bone Tissue Engineering. *BioMed Res. Int.* **2022**, 4996530. [[CrossRef](#)]
11. Padmanabhan, S.K.; Gervaso, F.; Carrozzo, M.; Scalera, F.; Sannino, A.; Licciulli, A. Wollastonite/hydroxyapatite scaffolds with improved mechanical, bioactive and biodegradable properties for bone tissue engineering. *Ceram. Int.* **2013**, *39*, 619–627. [[CrossRef](#)]

12. Srinath, P.; Abdul Azeem, P.; Venugopal Reddy, K. Review on calcium silicate-based bioceramics in bone tissue engineering. *Int. J. Appl. Ceram. Technol.* **2020**, *17*, 2450–2464. [[CrossRef](#)]
13. Morsy, R.; Abuelkhair, R.; Elnimr, T. A Facile Route to the Synthesis of Hydroxyapatite/Wollastonite Composite Powders by a Two-Step Coprecipitation Method. *Silicon* **2017**, *9*, 637–641. [[CrossRef](#)]
14. Lin, K.; Zhang, M.; Zhai, W.; Qu, H.; Chang, J. Fabrication and Characterization of Hydroxyapatite/Wollastonite Composite Bioceramics with Controllable Properties for Hard Tissue Repair. *J. Am. Ceram. Soc.* **2011**, *94*, 99–105. [[CrossRef](#)]
15. Hammood, A.S.; Hassan, S.S.; Alkhafagy, M.T.; Jaber, H.L. Effect of calcination temperature on characterization of natural hydroxyapatite prepared from carp fish bones. *SN Appl. Sci.* **2019**, *1*, 436. [[CrossRef](#)]
16. Zheng, Y.; Wang, C.; Zhou, S.; Luo, C. The self-gelation properties of calcined wollastonite powder. *Constr. Build. Mater.* **2021**, *290*, 123061. [[CrossRef](#)]
17. Y González-Barros, M.R.; García-Ten, J.; Alonso-Jiménez, A. Synthesis of wollastonite from diatomite-rich marls and its potential ceramic uses. *Bol. Soc. Española Ceram. Vidr.* **2022**, *61*, 585–594. [[CrossRef](#)]
18. Ribas, R.G.; Campos, T.M.B.; Schatkoski, V.M.; de Menezes, B.R.C.; Montanheiro, T.L.d.A.; Thim, G.P.  $\alpha$ -wollastonite crystallization at low temperature. *Ceram. Int.* **2020**, *46*, 6575–6580. [[CrossRef](#)]
19. Dermawan, S.K.; Ismail, Z.M.M.; Jaffri, M.Z.; Abdullah, H.Z. Effect of the Calcination Temperature on the Properties of Hydroxyapatite from Black Tilapia Fish Bone. *J. Phys. Conf. Ser. IOP* **2022**, *2169*, 012034. [[CrossRef](#)]
20. ASTM C1424-04; Standard Test Method for Monotonic Compressive Strength of Advanced Ceramics at Ambient Temperature. ASTM Committee: West Conshohocken, PA, USA, 2013.
21. Kokubo, T.; Kushitani, H.; Sakka, S.; Kitsugi, T.; Yamamuro, T. Solutions able to reproduce in vivo surface-structure changes in bioactive glass-ceramic A-W3. *J. Biomed. Mater. Res.* **1990**, *24*, 721–734. [[CrossRef](#)]
22. ISO 10993-12:2021; Biological Evaluation of Medical Devices—Part 12: Sample Preparation and Reference Materials, 5th ed. ISO: Geneva, Switzerland, 2021.
23. ISO 10993-5:2009; Biological Evaluation of Medical Devices—Part 5: Tests for In Vitro Cytotoxicity, 5th ed. ISO: Geneva, Switzerland, 2009.
24. Abere, D.V.; Ojo, S.A.; Oyatogun, G.M.; Paredes-Epinosa, M.B.; Niluxsshun, M.C.D.; Hakami, A. Mechanical and morphological characterization of nano-hydroxyapatite (nHA) for bone regeneration: A mini review. *Biomed. Eng. Adv.* **2022**, *4*, 100056. [[CrossRef](#)]
25. Goudouri, O.-M.; Balasubramanian, P.; Boccacini, A.R. 6—Characterizing the degradation behavior of bioceramic scaffolds. In *Characterisation and Design of Tissue Scaffolds*; Woodhead Publishing Series in Biomaterials: Cambridge, UK, 2016; pp. 127–147. [[CrossRef](#)]
26. Jiao, L.; Xiao, H.; Wang, Q.; Sun, J. Thermal degradation characteristics of rigid polyurethane foam and the volatile products analysis with TG-FTIR-MS. *Polym. Degrad. Stab.* **2013**, *98*, 2687–2696. [[CrossRef](#)]
27. Wang, H.; Tian, Y.; Li, J.; Chen, X. Experimental study on thermal effect and gas release laws of coal-polyurethane cooperative spontaneous combustion. *Sci. Rep.* **2021**, *11*, 1994. [[CrossRef](#)] [[PubMed](#)]
28. Abbasi, N.; Hamlet, S.; Love, R.M.; Nguyen, N.T. Porous scaffolds for bone regeneration. *J. Sci. Adv. Mater. Devices* **2020**, *5*, 1–9. [[CrossRef](#)]
29. Kaur, G.; Kumar, V.; Bains, B.; Mauro, J.C.; Pickrell, G.; Evans, I.; Bretcanu, O. Mechanical properties of bioactive glasses, ceramics, glass-ceramics and composites: State-of-the-art review and future challenges. *Mater. Sci. Eng. C* **2019**, *104*, 109895. [[CrossRef](#)] [[PubMed](#)]
30. Gibson, L.J.; Ashby, M.F. *Cellular Solids: Structure & Properties*, Oxford: Pergamon Press, ISBN: 0-08-036607-4, 1988, 357+ Ix Pages, \$35.00. *Adv. Polym. Technol.* **1989**, *9*, 165–166. [[CrossRef](#)]
31. Padmanabhan, S.K.; Carozzo, M.; Gervaso, F.; Scalera, F.; Sannino, A.; Licciulli, A. Mechanical Performance and In Vitro Studies of Hydroxyapatite/Wollastonite Scaffold for Bone Tissue Engineering. *Key Eng. Mater.* **2011**, *493–494*, 855–860. [[CrossRef](#)]
32. Nakamura, J.; Sugawara-Narutaki, A.; Ohtsuki, C. 16-Bioactive ceramics: Past and future. In *Bioceramics: From Macro to Nanoscale*; Elsevier Series on Advanced Ceramic Materials; Elsevier: Amsterdam, The Netherlands, 2021; pp. 377–388. [[CrossRef](#)]
33. Tavoni, M.; Dapporto, M.; Tampieri, A.; Sprio, S. Bioactive Calcium Phosphate-Based Composites for Bone Regeneration. *J. Compos. Sci.* **2021**, *5*, 227. [[CrossRef](#)]
34. Rabiee, S.M.; Nazparvar, N.; Azizian, M.; Vashae, D.; Tayebi, L. Effect of ion substitution on properties of bioactive glasses: A review. *Ceram. Int.* **2015**, *41*, 7241–7251. [[CrossRef](#)]
35. Rutkovskiy, A.; Stenslkken, K.O.; Vaage, I.J. Osteoblast Differentiation at a Glance. *Med. Sci. Monit. Basic Res.* **2016**, *22*, 95–106. [[CrossRef](#)]
36. Qian, G.; Zhang, L.; Wang, G.; Zhao, Z.; Peng, S.; Shuai, C. 3D Printed Zn-doped Mesoporous Silica-incorporated Poly-L-lactic Acid Scaffolds for Bone Repair. *Int. J. Bioprint.* **2021**, *7*, 346. [[CrossRef](#)]
37. Paun, I.A.; Popescu, R.C.; Mustaciosu, C.C.; Zamfirescu, M.; Calin, B.S.; Mihailescu, M.; Dinescu, M.; Popescu, A.; Chioibas, D.; Soproniy, M.; et al. Laser-direct writing by two-photon polymerization of 3D honeycomb-like structures for bone regeneration. *Biofabrication* **2018**, *10*, 025009. [[CrossRef](#)]

38. Paun, I.A.; Popescu, R.C.; Calin, B.S.; Mustaciosu, C.C.; Dinescu, M.; Luculescu, C.R. 3D Biomimetic Magnetic Structures for Static Magnetic Field Stimulation of Osteogenesis. *Int. J. Mol. Sci.* **2018**, *19*, 495. [[CrossRef](#)]
39. Balvan, J.; Krizova, A.; Gumulec, J.; Raudenska, M.; Sladek, Z.; Sedlackova, M.; Babula, P.; Sztalmachova, M.; Kizek, R.; Chmelik, R.; et al. Multimodal holographic microscopy: Distinction between apoptosis and oncosis. *PLoS ONE* **2015**, *10*, e0121674. [[CrossRef](#)]

**Disclaimer/Publisher's Note:** The statements, opinions and data contained in all publications are solely those of the individual author(s) and contributor(s) and not of MDPI and/or the editor(s). MDPI and/or the editor(s) disclaim responsibility for any injury to people or property resulting from any ideas, methods, instructions or products referred to in the content.